Preparation of a Silica/Poly(*n*-butyl acrylate-*co*-acrylic acid) Composite Latex and Its Pressure-Sensitive Properties

Nongyue Wang,[1] Yakun Guo,[1] Hongping Xu,[2] Xinran Liu,[1] Liqun Zhang,[3] Xiongwei Qu,[1] Liucheng Zhang[1]

[1]*Institute of Polymer Science and Engineering, School of Chemical Engineering, Hebei University of Technology, Tianjin 300130, People's Republic of China*
[2]*Zhejiang University of Radio and Television, Xiaoshan College, Xiaoshan 311201, People's Republic of China*
[3]*Beijing University of Chemical Technology, Beijing 100029, People's Republic of China*

Received 30 April 2008; accepted 28 February 2009
DOI 10.1002/app.30348
Published online 4 May 2009 in Wiley InterScience (www.interscience.wiley.com).

ABSTRACT: Silica with an average particle size of 125 nm was prepared by the sol–gel reaction of tetraethoxysilane with a base catalyst and then modified with a vinyl-functionalized silane [γ-methacryloxypropyl trimethoxysilane (MPS)]. The composite latex, with the modified silica as the core and poly(*n*-butyl acrylate-*co*-acrylic acid) [poly(BA-*co*-AA)] polymer as the shell, was synthesized by a semicontinuous emulsion polymerization and used as a pressure-sensitive adhesive. The structures were characterized by Fourier transform infrared spectrometry, X-ray photoelectron spectroscopy, elemental analysis, and transmission electron microscopy. The particle sizes of the silica and MPS-modified silica (MPS–silica)/poly(BA-*co*-AA) composite latexes were determined by dynamic light scattering in a semicontinuous emulsion polymerization online. The monomers of *n*-butyl acrylate and acrylic acid grew around the MPS–silica particles without significant secondary nucleation, and the composite latexes exhibited a core–shell structure with the modified silica particles enwrapped in poly(BA-*co*-AA). To compare the adhesion properties, including the loop tack force, peel strength, and shear resistance, by Fédération Internationale des Fabricants et Transformateurs d'Adhésifs et Thermocollants sur Papiers et Autres Supports test methods, poly(methyl methacrylate-*co*-allyl methacrylate)/poly(BA-*co*-AA) latex and the full poly(BA-*co*-AA) latex were prepared with the same particle size and the same emulsion polymerization process. The shear resistance of the composite latex film greatly increased after the addition of the silica to the core of the poly(BA-*co*-AA) latex. The relationships between the adhesive properties and the different structures in the core components were examined. © 2009 Wiley Periodicals, Inc. J Appl Polym Sci 113: 3113–3124, 2009

Key words: adhesives; core-shell polymers; emulsion polymerization; silicas; structure–property relations

INTRODUCTION

Pressure-sensitive adhesives (PSAs) are viscoelastic materials that can adhere strongly to solid surfaces upon application of light contact pressure for a short contact time.[1] Emulsion polymerization as a technology for PSA production offers better environmental compliance compared to solvent technology and better energy efficiency compared to hot-melt technology. More than 40% of adhesives on the global market are waterborne adhesives.[2] Polyacrylates are transparent and colorless, and because they are saturated, they are very resistant to oxidation and do not yellow on exposure to sunlight. They have enjoyed the fastest growth and biggest share of the PSA market in commercial applications.[3] However, because acrylic PSAs comprise polymers that have high entanglement molecular weight (M_e) values, low glass-transition temperature (T_g) values, and medium to low molecular weights, some types of crosslinking must be provided to yield shear holding power.[4–6] In fact, neat acrylic latexes are hardly used

Correspondence to: X. Qu (xwqu@hebut.edu.cn).

Contract grant sponsor: Key Project of the Natural Science Foundation of Hebei Province; contract grant number: E2007000077.
Contract grant sponsor: Research Foundation of the Key Laboratory for Nanomaterials of the Ministry of Education of China; contract grant number: 2007-2.
Contract grant sponsor: Excellent Project of the Ministry of Personal Resources of China; contract grant number: 2006-164.
Contract grant sponsor: Start-Up Foundation of the Ministry of Education of China; contract grant number: 2007-24.
Contract grant sponsor: Research Foundation of the Key Laboratory of Beijing City for the Preparation and Processing of Novel Polymer Materials; contract grant number: 2006-1.
Contract grant sponsor: Distinguished Young Scientist of the National Science Foundation; contract grant number: 50725310.

as PSAs because of their low shear resistance, although intraparticle crosslinking occurs as part of the chain transfer to the polymer during emulsion polymerization.[7,8] A balanced combination of tack, peel strength, and shear resistance is of primary concern in PSA production. Howard[9] stated that, along with the replacement of solvent-based systems with waterborne or solventless adhesives, the future would bring the development of hybrid adhesive systems and custom-designed products.

The combination of organic polymers and inorganic particles into nanocomposites has attracted considerable attention in recent years, as these materials offer the prospect of new synergetic properties that originate from their organic and inorganic components.[10–13] Organic/inorganic particles can be produced by a variety of ways with either *ex situ* or *in situ* techniques. Among the number of inorganic/organic materials, silica/polymer composite materials, because of their potential use as aerospace materials, structural materials in electronics, sensors, and materials in other industries, have attracted considerable interest.[14–18] Until now, although much research has been done on the preparation of silica/polymer composite materials, latexes with composite structures have not yet been used as PSAs, and the effect of the introduction of silica on the adhesive properties has not been studied to our knowledge. In this article, we report on the synthesis of a modified silica/poly(*n*-butyl acrylate-*co*-acrylic acid) [poly(BA-*co*-AA)] composite latex through semicontinuous emulsion polymerization with an *in situ* method. Silica particles with an average size of 125 nm were first obtained via the Stöber and Fink[19] method. Organic modification of the silica particles was performed by the grafting of organosilane molecules, γ-methacryloxypropyl trimethoxysilane (MPS), bearing a reactive vinyl group. The MPS-modified silica (MPS–silica) was preemulsified in the presence of water and surfactant and then polymerized with acrylic monomers in an emulsion. Their morphology and particle size were systemically characterized. The pressure-sensitive properties were investigated with Fédération Internationale des Fabricants et Transformateurs d'Adhésifs et Thermocollants sur Papiers et Autres Supports test methods and compared with others with poly(*n*-butyl acrylate) [poly(BA)] and crosslinked poly(methyl methacrylate) [poly(MMA)] as core layers.

EXPERIMENTAL

Materials

tert-Dodecyl mercaptan (TDM; Merck, Hohenbrunn, Germany) and the anionic surfactant, Aerosol Series (Cytec, Rotterdam, Netherlands), were used as supplied. Potassium persulfate (KPS), tetraethyl orthosilicate (TEOS), absolute ethanol (EtOH), and ammonia (NH_4OH) solution (25 wt %) are purchased from Tianjin Chemical Reagent Co. of China (Nanjing City, China). MPS was purchased from Nanjing Shuguang Chemical Co. of China (Beijing City, China). All of these materials are used without further purification. *n*-Butyl acrylate (BA), acrylic acid (AA; 99%), and methyl methacrylate (MMA) were purchased from Beijing Dongfang Chemical Co. of China (Beijing City, China). Allyl methacrylate (ALMA), purchased from Tianjiao Chemical Co. of China (Tianjin City, China), was used as received. The BA monomer was freed of inhibitor by washing with a 2% NaOH solution; it was then washed with deionized water until the washed waters were neutral and finally dried with $CaCl_2$ overnight, after which it was distilled under reduced pressure. MMA and AA were purified by distillation under reduced pressure before use. Hydroquinone (99%) was used as an inhibitor of the latexes taken from the emulsion polymerization procedure. Deionized water was used for all polymerization and treatment processes.

Preparation and modification of silica

The Stöber method is a well-known process for synthesizing narrowly dispersed silica particles.[19] EtOH was used as a reaction medium, NH_4OH was used as a catalyst, and TEOS was used as a reacting agent. The reactants were charged into a 500-mL, three-necked bottom flask equipped with a mechanical stirrer, thermometer, and condenser according to an initial volume ratio of 15 : 250 : 15 TEOS/EtOH/NH_4OH. EtOH and NH_4OH were mixed for 5 min, and then, TEOS was dropped in after 2 h at 40°C in a water bath, with the reaction kept for another 4 h to complete the procedure.

Silicas (4.8 g) were charged into a 500-mL, four-necked flask equipped with a mechanical stirrer, thermometer, and reflux condenser. A mixture of the weighted MPS (0.009–0.176 g) with 3 g of water and 7 g of EtOH was sonicated for 10 min to promote the hydrolyzation reaction of MPS. The solution was dropped into the flask for 1.5 h with stirring at 50°C, and then the reaction was kept for another 24 h. Afterward, the products were collected by centrifugation and filtration. All MPS–silica particles were washed several times with EtOH, dried, extracted with toluene for 24 h to remove the excessively absorbed silane and other impurities, and then dried at 80°C *in vacuo* for 24 h.

Preparation of the MPS–silica/poly(BA-*co*-AA) composite latex, the poly(methyl methacrylate-*co*-allyl methacrylate) [poly(MMA-*co*-ALMA)]/poly(BA-*co*-AA) latex, and the full poly(BA-*co*-AA) latex

The synthesis of the MPS–silica/poly(BA-*co*-AA) composite latex was carried out in a 3-L, four-

TABLE I
Formulation for the Preparation of (A) the MPS–Silica/Poly(BA-*co*-AA) Composite Latex, (B) the Poly(MMA-*co*-ALMA)/Poly(BA-*co*-AA) Latex, and (C) the Full Poly(BA-*co*-AA) Latex

Stage	Component	A (g)	B (g)	C (g)
Seed stage	Deionized water	900.0	700	700
	Surfactant	1.34	2.67	0.86
	MPS–silica	40.0	—	—
	KPS/deionized water	1.25/50	2.80/150	2.80/150
	MMA	—	25	—
	ALMA	—	0.32	—
	BA	—	—	25
Growth stage	BA	575.5	935	935
	AA	17.0	27.65	27.65
	Surfactant	8.30	11.90	11.90
	TDM	0.21	0.34	0.34
	KPS/deionized water	0.80/150	0.68/150	0.68/150

necked, flanged reaction flask equipped with a condenser, nitrogen inlet, mechanical stirrer, and thermometer. The amounts used for the preparation of the latex are listed in Table I (column A). The MPS–silica, surfactant and deionized water, as indicated at the seed stage, were preemulsified under vigorous stirring and sonication dispersion for 1 h and then heated to 80°C to start the emulsion polymerization by the addition of KPS solution. This corresponded to time zero for the polymerization, which was followed by the dropping of the mixture of ingredients at the growth stage, as listed in Table I, for 3 h. After the following completion of the addition of the growth-stage reactant mixture, another 60 min was allowed before the latex was cooled to room temperature and filtered through a 53-μm sieve to obtain the coagulum content. The same method described previously, except for the seed stage, was used to prepare the poly(MMA-*co*-ALMA)/poly(BA-*co*-AA) latex and the full poly(BA-*co*-AA) latex. The recipes are also listed in Table I (columns B and C, respectively). The solid content for the MPS–silica/poly(BA-*co*-AA) composite latex was 36.32%, and the latex was rotary-film-evaporated to increase its solid content to 50%. The solid contents for the poly(MMA-*co*-AA)/poly(BA-*co*-AA) and full poly(BA-*co*-AA) latexes were nearly 50%. The coatings of 50% solid content latexes are of a high quality to be used for adhesive testing. NH_4OH (25 wt %) was added to the reactor to increase the pH value to 5.5 to enhance the latex shear and shelf stability. The amount of residual monomer was measured with gas chromatography/mass spectrometry and was about 0.6–1.0% on the basis of the wet latex weight.

Characterization

A Bruker (Burladingen, Germany) Vector-22 Fourier transform infrared (FTIR) apparatus was used to characterize the silica particles with KBr pellets. X-ray photoelectron spectroscopy (XPS) images of the silica and the MPS–silica were collected with an ESCALAB 250 apparatus (Thermo Electron, Waltham, MA) to illuminate the interaction between the particles and the grafted silane coupling agent. Elemental analysis (Thermo Electron CHNSO) was used to analyze the chemical composition on the surface modification of the silicas with different contents of the MPS silane coupling agent.

The monomer-to-polymer conversions were determined gravimetrically. At 30-min intervals, samples (10 mL) were removed from the reaction flask with a syringe to evaluate the variation of particle diameter and percentage conversion with reaction time. The polymerization was short-stopped with hydroquinone to prevent any further polymerization. The products were dried until a constant weight was reached under reduced pressure in an oven at 60°C. The overall conversion was equal to the ratio between the weights of the polymer formed in the reactor and the total amount of monomer added. The instantaneous monomer conversion was equal to the ratio between the weight of polymer formed in the reactor and the total amount of monomer that was added. The details are described in ref. 20. The particle sizes and distributions of the synthesized silica, the MPS–silica/poly(BA-*co*-AA) composite latex (also called PSA–silica), the poly(MMA-*co*-ALMA)/poly(BA-*co*-AA) latex (also called PSA–MMA), and the full poly(BA-*co*-AA) latex (also called PSA–BA) were measured at 633 nm with a dynamic light scattering (DLS) instrument manufactured by Malvern Instruments (Worcestershire, UK) (Zetasizer 3000HS) with the configuration of a 90° scattering angle. The analyses were carried out at 25 ± 0.1°C. Three measurements were carried out for each sample, and a mean value of the *z*-average particle diameter was calculated. Transmission electron microscopy (TEM; Philips TECNAI F20, Blackwood, NJ) was used to visualize the morphology of the silica and the MPS–silica/poly(BA-*co*-AA) composite latex. The samples were dispersed in water sufficiently with ultrasonic waves before characterization and were then prepared by the casting of one drop of diluted solution onto a carbon-coated copper grid.

The dynamic mechanical properties, including the storage modulus and damping (tan δ) of the MPS–silica/poly(BA-*co*-AA), poly(MMA-*co*-AA)/poly(BA-*co*-AA), and the full poly(BA-*co*-AA) PSAs were obtained with a Triton 2000 (Leeuwerikstraat, Belgium) dynamic mechanical analyzer in the plate clamp mode. The plate sample with typical

dimensions of 10 × 5 × 2 mm^3 was prepared through cast molding. The heating rate and frequency were 5°C/min and 1 Hz, respectively. Thermogravimetric analysis (TGA) of the dried gels was performed with a TGA 951 (DuPont Instruments, New Castle, DE) under a nitrogen atmosphere at a heating rate of 10°C/min.

The latexes are coated with an Elcometer 4360/15 bar onto 36 μm thick poly(ethylene terephthalate) (PET) to give a 30 μm dry film thickness (Jiffy Packaging Company Limited, Winsford, UK). A temperature of 105°C for 4 min was used to dry the composite latex. The PSA testing was done at 23°C and 50% relative humidity, and the samples were climatized to this condition for 24 h before testing. Loop tack and 180° peel were done off of a stainless steel substrate. The test methods were in accordance with the Fédération Internationale des Fabricants et Transformateurs d'Adhésifs et Thermocollants sur Papiers et Autres Supports test methods 9 and 1 at 300 mm/min on an Instron (USA) 1122 tester. The maximum force of detachment was recorded as loop tack. The average of the three middle peeling forces was recorded. Shear resistance was done off of a glass plate substrate with a 25 × 25 mm^2 PET-coated strip and a 1000-g hanging weight according to Fédération Internationale des Fabricants et Transformateurs d'Adhésifs et Thermocollants sur Papiers et Autres Supports test method 8. The data given are the average of three trials.

RESULTS AND DISCUSSION

Preparation of the silica and modification of the silica with MPS

Figure 1 presents the particle size distributions of the original silica, MPS–silica, and MPS–silica/poly(BA-*co*-AA) latex particles at different polymerization times as measured by DLS. The curves, noted as 1 and 2 in Figure 1, were the results for the original silica and MPS–silica, respectively. The *z*-average hydrodynamic diameter was 142 nm for the MPS–silica particles, and the distribution index was 0.058. Figure 2 shows the TEM image of the MPS–silica particles. It was analyzed to determine the mean diameter, and the distribution of the MPS–silica particles was analyzed by an image analyzer. An average of 300 diameter measurements was obtained. The number-average diameter (D_n) was calculated from the following equation:

$$D_n = \frac{\sum N_i D_i}{\sum N_i}$$

where N_i is the number of particles with diameter D_i.

The mean diameter of the MPS–silica particles was 139 nm, and the frequency diagram of the particle diameter obtained by TEM is shown in

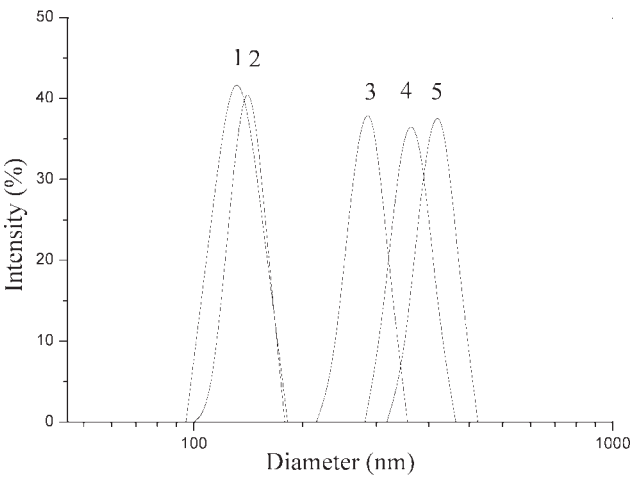

Figure 1 Particle diameter distributions of the MPS–silica and MPS–silica/poly(BA-*co*-AA) composite latexes at different growth stages: (1) −60 min (silica), (2) 0 min (MPS–silica) and (3) 60, (4) 120, and (5) 240 min.

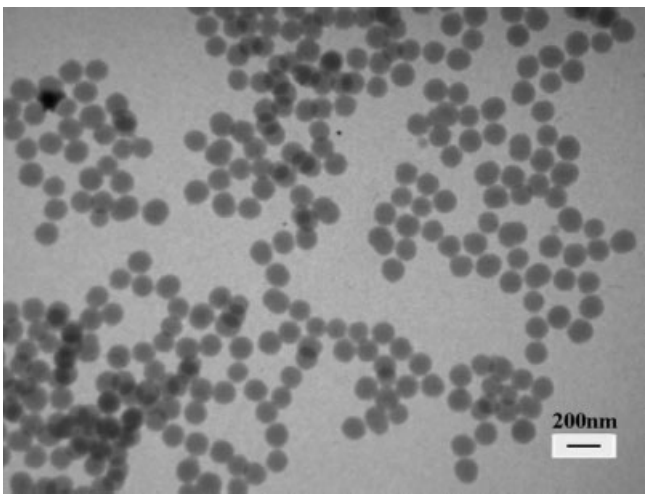

Figure 2 TEM image of the MPS–silica particles.

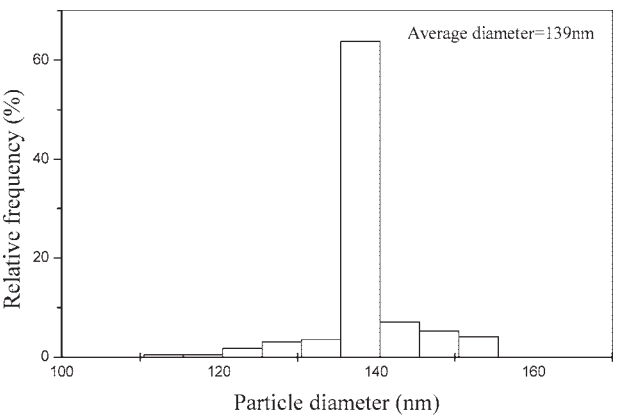

Figure 3 Frequency diagram of the diameter distribution of the MPS–silicas obtained by TEM.

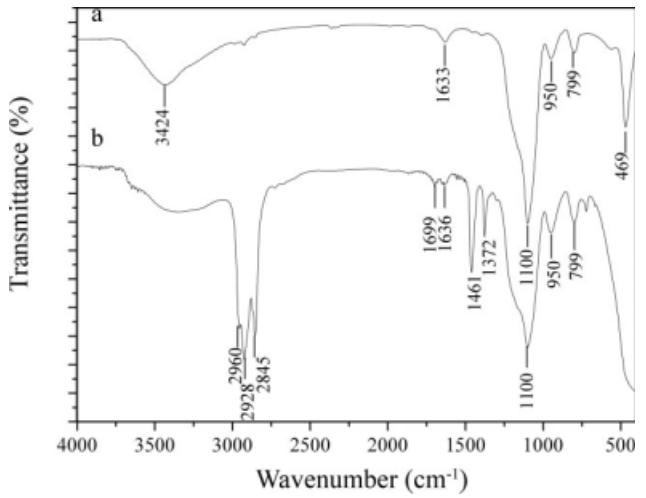

Figure 4 FTIR spectra of the (a) silica and (b) MPS–silica.

Figure 3. From the observation of TEM and DLS measurements, the modified silicas were spherical particles with narrow distribution.

The anchoring of alkoxysilanes onto the surface of the silica particles was obtained by condensation reactions between OH— groups present on the oxide surface and silanol groups formed by the hydrolysis of the alkoxysilanes. Therefore, the grafting reactions could be easily identified by means of the simultaneous disappearance of bands assigned to the various functional groups of silane (e.g., methoxy or ethoxy functions) and silanol groups on the silica particles. To gain a better understanding of the formation of silica and the grafting process of MPS onto the silica surface, the FTIR spectra helped to confirm their structures. Figure 4 illustrates the FTIR spectra of the silica and MPS–silica. The adsorption bands shown in Figure 4(a,b) were similar; that is, there were characteristic peaks at about 1100, 950, and 799 cm^{-1} assigned to the stretching vibrations of Si—O—Si. The peaks at 2960, 2928, and 2845 cm^{-1} were assigned to the asymmetric stretching of CH_3, the asymmetric stretching of CH_2 and the symmetric CH_3, respectively. An absorption corresponding to the H—O—H bending vibration, 1636 cm^{-1}, was also found; this indicated that residual intramolecular waters existed within the silicas. There was also an absorption band of C=O at 1699 cm^{-1} for the modified silica, as indicated in Figure 4(b), but no such an absorption is shown sin Figure 4(a). Another significant phenomenon was the absorption at 3424 cm^{-1}, which showed that the stretching mode of —OH became weak in the modified version. As the MPS–silica sample was extracted by Soxhlet extraction with toluene, the physically absorbed MPS was removed. In the grafting process, silane coupling agents were first hydrolyzed to form an organosilanetriol and then organosilanetriol, which reacted with —OH on the surface of the silica to form Si—O—Si bonds. This indicated that part of the hydroxyl groups on the surface of the silica reacted with MPS and, consequently, caused the number of hydroxyls to decrease.

The extracted MPS–silica was characterized by XPS, with the original version as a control (MPS content = 4 wt %). From the XPS spectra, as shown in Figure 5, we determined that the binding energies of Si2s and Si2p in the modified version were 159.9 and 108.8 eV, respectively, whereas they were 160.5 and 109.2 eV, respectively, in the original version. There were 0.6- and 0.4-eV shifts to the low binding energies after the silica particles were modified. This shift was caused by changes in the chemical environments where the atoms existed. Electrons around C—O transferred to O—Si because of the weaker electronegativity of silicon than that of carbon. Hence, the electronic density around the silicon atoms increased, which caused the binding energy to become lower. Meanwhile, the binding energy of

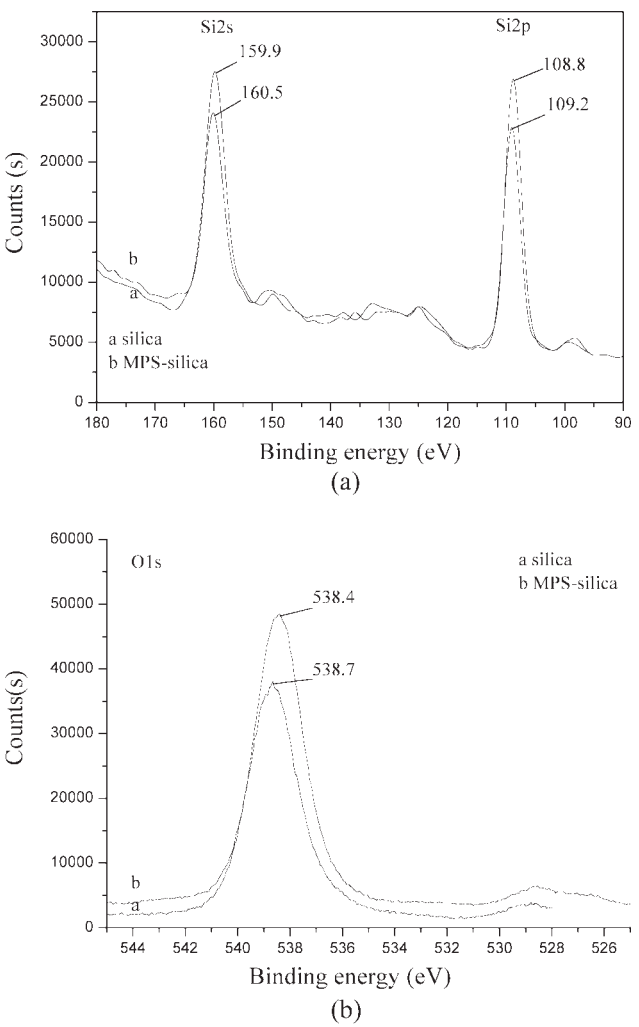

Figure 5 XPS spectra of the silica before and after modification by MPS: (a) XPS Si2s and (b) XPS O1s.

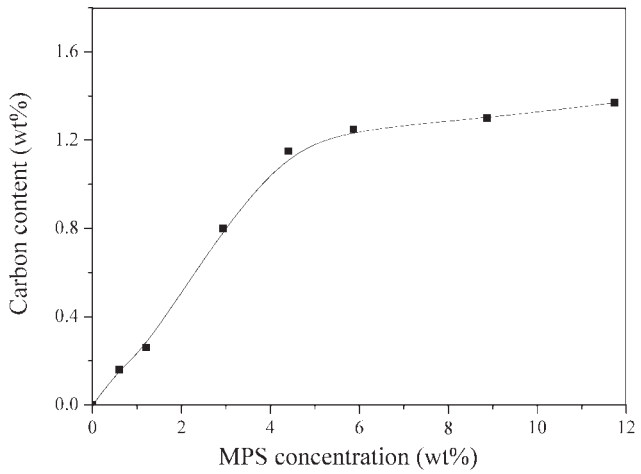

Figure 6 Variation of the carbon content on the silica surface with the MPS concentration.

O1s in the modified version was also lower than the original version. Both the FTIR and XPS spectra revealed that the MPS molecules were effectively grafted onto the surface of the silica particles.

The amount of grafted MPS on the silica surface was determined by elemental analysis data based on the elemental carbon accounting for the overall sample percentage. Figure 6 shows the evolution of the MPS grafting percentage as a function of the initial MPS concentration. The grafting percentage increased with the increase of the silane content and leveled off after the addition of MPS content over 4 wt %. This result was well corroborated when we took into account the steric hindrance caused by an MPS unit at the silica surface. It was probable that the organic grafting at the particle surface provided a decisive contribution to the preparation of the modified silica/poly(BA-*co*-AA) composite latex. Therefore, the 4 wt % MPS content to modify the silica surface was used from the cost, and this modification resulted in the following semicontinuous polymerization of the MPS–silica composite latex.

Preparation and characterization of the MPS–silica/poly(BA-*co*-AA) composite latex

The samples removed from the emulsion polymerization contained volatile materials (unreacted monomer and water) and nonvolatile materials (polymer, surfactant, and initiator). The conversion of the volatile monomer into nonvolatile polymer, therefore, could be monitored by the measurement of the latex solid content. The levels of coagulum for the MPS–silica/poly(BA-*co*-AA) composite latex were less than 1.0 wt %; hence, the use of solid content to evaluate the monomer conversion was valid. The overall and instantaneous conversions were calculated for each of the aliquots taken with a mass balance approach. Figure 7(a) shows conversion–time data for the MPS–silica/poly(BA-*co*-AA) composite latex preparation. As the reaction proceeded from 60 to 180 min, the instantaneous conversion was around 90%. Under these conditions, the copolymer composition was uniform and approximately equal to the composition of the BA/AA comonomer feed mixture. The high final conversion (98.47 wt %) meant that only small amounts of residual comonomer were present in the final latexes. This is an important factor because any residual monomer can behave as a plasticizer, which will affect the adhesive properties.

The DLS technique is used to provide a rapid means of monitoring the particle size of latex particles. With this information, it is possible not only to establish and reproduce a latex system of known particle diameter but also to determine whether, during the growth stage of polymerization, the latex particles grow sequentially or whether secondary nucleation occurs. Figure 7(b) shows the variation of

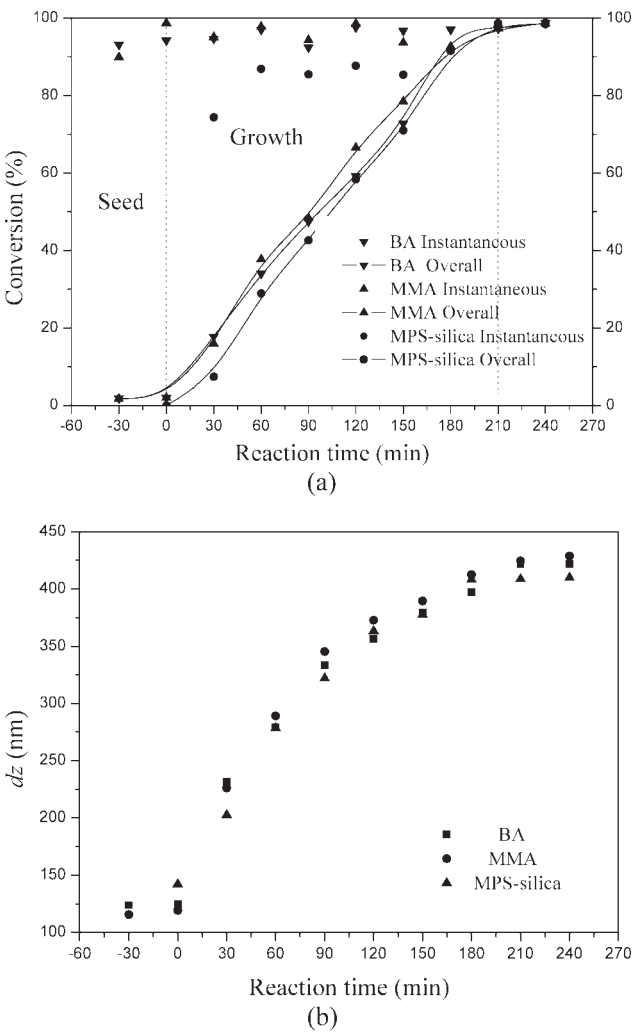

Figure 7 Variation with the reaction time of the (a) overall and instantaneous conversion and (b) measured *z*-average particle diameter (d_z) with different types of core layers.

TABLE II
Particle Sizes and PDIs of the MPS–Silica/Poly(BA-*co*-AA) Composite Latexes at Different Reaction Times

Reaction time (min)	Particle size (nm)		PDI
	Predicted	Measured	
−60	—	125	0.018
0	142	142	0.058
60	288	278	0.077
120	366	363	0.075
240	420	410	0.091

particle size in the prepared latex with reaction time. Figure 1 tracks the particle size dispersion profiles at the different growth stages in the semicontinuous emulsion polymerization (noted as 3, 4, and 5 in Fig. 1, which correspond to reaction times of 60, 120, and 240 min, respectively). Table II summarizes the particle diameters and particle distribution indices (PDIs) at the initial stage and growth stage. Figures 2 and 7(b) and Table II demonstrate that the particle sizes of the MPS–silica/poly(BA-*co*-AA) latexes increased with the addition of the mixture of BA and AA monomers, and their particle size distributions were also narrow. Meanwhile, the theoretical values of the *z*-average particle diameter for particles during the growth stage were calculated from the measured value of the MPS–silica at the end of the seeded stage, the density of poly(BA-*co*-AA) polymer, and the instantaneous percentage conversion, with the assumption that the particles grew without significant secondary nucleation and were not swollen by unreacted monomer.[20] The data for the predicted and measured particle sizes are also listed in Table II. The data from the prediction were theoretically consistent with those measured. Therefore, the polymerization in the presence of MPS–silica proceeded under monomer-starved conditions and with good control of particle growth without secondary nucleation, as evidenced by good agreement between the measured and theoretical particle sizes. This result was also confirmed by TEM observation.

The morphology of the MPS–silica/poly(BA-*co*-AA) composite latex was observed by TEM, as shown in Figure 8. The particle consisted of a dark core, which was silicon dioxide, and a brighter shell, which was the polymer. All of the composite latex particles exhibited core–shell structures, and every latex particle contained only a single MPS–silica particle. The image indicated that the particles of the modified silica were mainly separated and covered by the polymer. The particle size determined by TEM was close to that determined by DLS. The morphology of this composite latex might have possibly been formed by the following mechanism: the monomer molecules of BA and AA and surfactant were adsorbed onto the surface of the hydrophobic MPS–silica, and the surfactants acted as micelles to ensure the that polymerization took place around the silica. In the presence of MPS–silica, some chemical interaction occurred, and covalent bonds were formed, as described by the FTIR and XPS characterizations. It was indicated that MPS molecules grafted onto the silica particles reacted with vinyl monomers via free-radical polymerization, which enhanced the effect of polymer encapsulation of the silica particles and improved the compatibility between the polymer and silica. There was no secondary nucleation in the growth stage after the addition of the mixture of the BA and AA monomers. Therefore, the latex showed more affinity for the silica surface with the poly(BA-*co*-AA) copolymer, which indicated that the organic modification was essential to the yield of a well-defined composite particle morphology.

Comparison of the latex growth process with the different core components

For the comparison of the adhesive properties of the prepared MPS–silica/poly(BA-*co*-AA) composite latex, we synthesized two other kinds of latex with the same particle size and the same emulsion polymerization using a relatively soft core, poly(BA), and a hard core, poly(MMA-*co*-ALMA). Figure 7 also shows the variation of the conversion with reaction time and the variation of particle size in the whole polymerization process. The main differences was in the instantaneous conversion for the composite latex, which might have been caused in the adsorption process for the BA and AA monomers around the MPS–silica particles, whereas the differences in particle size were also the same. A summary of the final latex factors with the different core components is

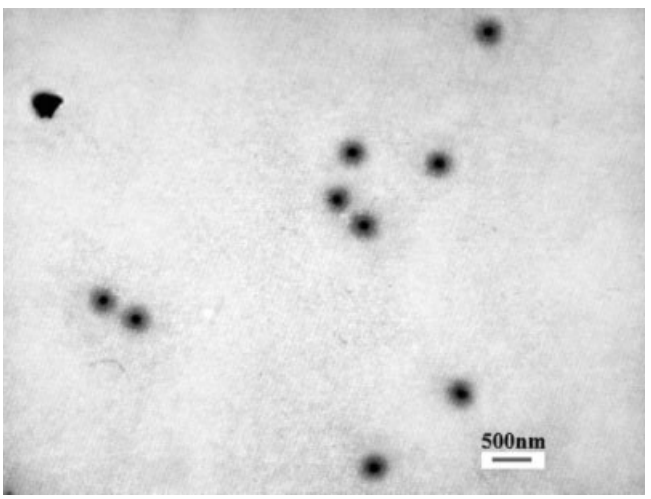

Figure 8 TEM image of the final MPS–silica/poly(BA-*co*-AA) composite latex particles.

TABLE III
Summaries of Some Parameters of the Final Latexes Prepared with Different Types of Core Components

Core	Overall conversion (wt %)	Coagulation (wt %)	Particle size at the end of the seed stage (nm)	Final particle size (nm)		PDI
				Theoretical	Measured	
BA	98.73	0.58	125	430	422	0.016
MMA	98.65	0.42	119	435	429	0.037
MPS–silica	98.47	0.97	142	420	410	0.091

listed in Table III. Regardless of which kinds of core components were used, the particle sizes at the end of the seed stage and the final latex particle size at the end of the growth stage were also the same. The theoretical particle sizes were in agreement with the measured ones. These results show that, during the growth stages, the particles grew under monomer-starved conditions. In the next section, we just consider the effects of the core components on the thermal, mechanical, and adhesive properties.

Thermal properties

It was proposed that a polymer resin reinforced with nanosized inorganic particulates would improve its thermal stability, including the resistances of thermal degradation and flammability. Therefore, we wished to estimate the resistance of thermal degradation of the current PSAs. Figure 9 shows the TGA and differential thermogravimetry (DTG) results. The temperature corresponding to a 5 wt % loss (T_5) was defined as the initial thermally degraded temperature of the copolymer phase. The T_5 values for PSA–BA, PSA–MMA, and PSA–MPS–silica were almost the same, being 343°C, whereas the semidecomposition temperatures (at 50 wt % loss) showed significant differences, being 393, 396, and 416°C for PSA–BA, PSA–MMA, and PSA–MPS–silica, respectively. The degradation temperature of the PSA increased with the addition of the silicas in the core of the core–shell polymers for the PSA materials.

Dynamic mechanical analysis (DMA)

The differences in the dynamic mechanical properties of PSA–BA, PSA–MMA, and PSA–silica were shown in the results of the DMA spectra of the films cast from the latexes because DMA is a sensitive thermal analytical technique for detecting transitions associated with molecular motions within polymers in the bulk state. The storage modulus and tan δ versus the temperature of the three types of PSAs are shown in Figure 10. The damping peak positions, corresponding to the T_g and tan δ values, were not changed. The peak width in the tan δ/temperature curve became narrow for PSA–silica. This also confirmed the homogeneous dispersion of MPS–silica in the continuous phase of poly(BA-*co*-AA). The data from the DMA curves are listed in Table IV. The storage modulus in the range of the scanning temperatures was ranked according to the magnitude of modulus in the core layer and increased from poly(BA) to crosslinked poly(MMA) to silica.

Another utility of DMA data is the determination of M_e. M_e can be estimated from the rubbery plateau modulus (G_N^o) as follows:[21]

$$M_e = \frac{\rho_p RT}{G_N^o}(1 + 2.5c + 14.1c^2)$$

where ρ_p is the density of the polymer [poly(BA)], R is 8.31×10^7 dyne cm mol^{-1} K^{-1}, T is the absolute temperature (K) at which G_N^o is located, G_N^o is determined from the location at which tan δ is at its minimum after the prominent peak, and c is the filler [poly(MMA) or silica] volume fraction. For crosslinked PSA, it was determined as a point of inflection in the tan δ curve after the prominent maximum. The values of T_g, G_N^o and its corresponding temperature, and M_e are also listed in Table IV.

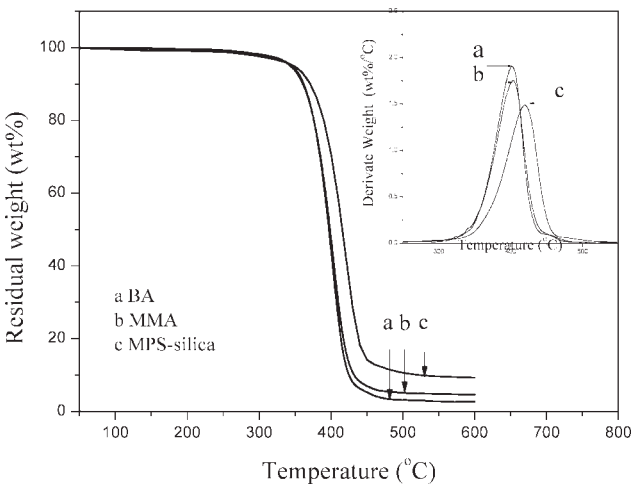

Figure 9 TGA and DTG curves of composite particles with different types of core components.

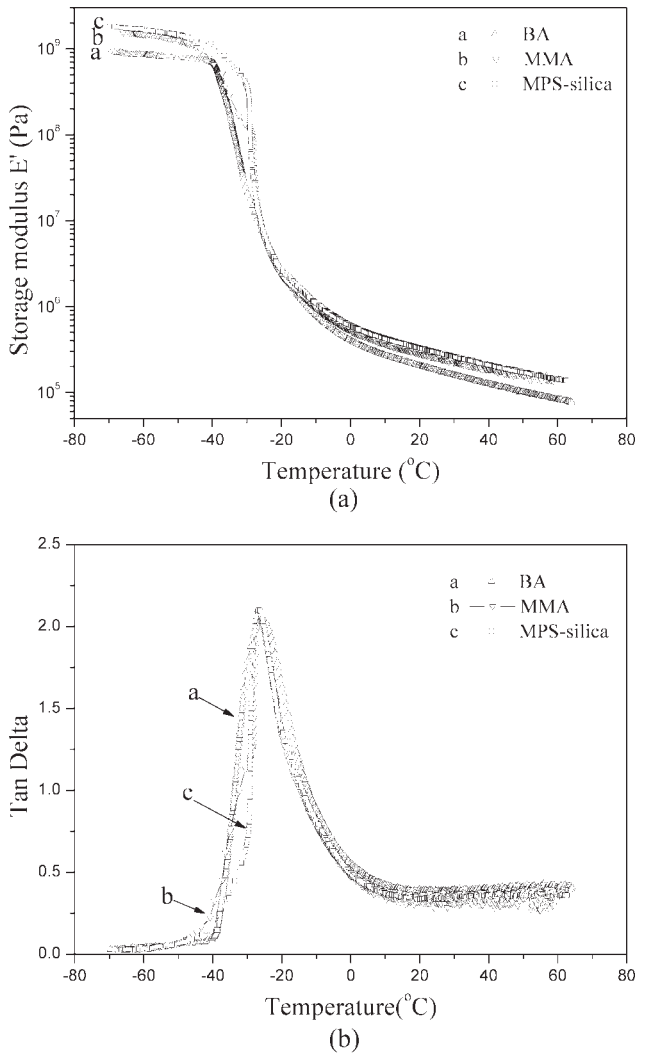

Figure 10 DMA spectra of the PSAs: (a) storage modulus and (b) tan δ.

Adhesive properties

The tack, peel strength, and shear strength are the three general adhesive properties that determine PSA performance. They are measured from steel or glass substrates. The results of the adhesive properties for the poly(BA-*co*-AA) PSAs with different core components are listed in Table V. As shown by the data in Table V, an extremely large increase in the shear resistance was achieved from 330 or 420 to 1500 min, when the core of the poly(BA) or poly-(MMA-*co*-ALMA) was replaced with the MPS–silica one, whereas the loop tack and peel adhesion remained at relatively high values.

The shear resistance of an adhesive is that which resists flowing or creeping. This property is of great importance in PSA applications. Shear resistance is assessed under conditions of static loading. The mechanism of bond failure must be in the bulk of the adhesive and not at the interface for the test to be a measure of cohesive strength. The gel contents for the three types of PSAs from Soxhlet extraction with boiling tetrahydrofuran were nearly the same within experimental error, as listed in Table IV. This was because the copolymer produced during the emulsion polymerization was of the same initial monomer feed composition at the growth stage.

The different behaviors of these three PSAs during the dynamic loading provided more evidence to explain the structural differences among PSA–silica, PSA–MMA, and PSA–BA. The silica particles had a high modulus and tensile strength. After they were modified with MPS organic molecules, which interconnected the silica particles through chemical bonding and correlated the grafted silica particles with the poly(BA-*co*-AA) shell layer, the dispersed particles presented good compatibility with the continuous phase, and a thick gradient layer was formed. Although the latexes with different core components were the same size, PSA–silica had the highest modulus, and the core–shell interface between MPS–silica and the poly(BA-*co*-AA) polymer was connected firmly. The thick gradient layer formed provided an effective bridge for the continuous phase to pass the stress to inorganic particles. The inclusion of hard microdomains in the soft continuous phase increased the film's tensile strength, which meant improved cohesive strength in the material.[22] For optimum tack and adhesion, a PSA must not be too stiff and must be able to dissipate energy during deformation. An excessively high storage modulus, relative to the dissipative character of the adhesive, would induce interfacial crack propagation.[23] Therefore, stress could be transferred to all the rigid particles when the film was subjected to an applied force, and this led to the increase of the cohesion strength and the shear resistance. As the mode of failure was cohesive for all tests, this approach for

TABLE IV
Values of T_g, Storage Modulus at 23°C, G_N^o and Its Corresponding Temperature, Gel Content, and M_e for PSA Films with Different Core Components

Core component	T_g (°C)	Storage modulus (Pa)	G_N^o (Pa)	Temperature (K)	Gel content (wt %)	M_e (g/mol)
BA	−25.7	1.79×10^5	7.13×10^4	291.75	70.46	36.1 K
MMA	−25.9	2.25×10^5	1.08×10^5	287.15	71.25	24.7 K
MPS–silica	−25.3	3.05×10^5	1.31×10^5	287.55	71.94	21.0 K

TABLE V
Adhesive Properties of PSAs with Different Core Components

Core component	Shear resistance (min/25 × 25 mm^2)	Tack force (N/25 mm)	180° peel force (N/25 mm)	
			20 min	24 h
BA	330	5.15	11.17	17.63
MMA	420	7.12	10.35	23.04
MPS–silica	1500	5.78	8.13	14.25

improving the cohesive strength was shown to be very effective in independently increasing PSA shear resistance without negatively affecting its peel adhesion, as discussed later. We propose that this effect was due to an additional mechanism of energy dissipation during shearing, which is thought to have involved the debonding of the filler from the polymer matrix. The mechanical behavior in the temperature range above T_g was governed by molecular entanglements.[21] Lowering the molecular weight between entanglements would create an adhesive with greater cohesive strength. The holding time depends on the internal structural resistance of the PSA to a shear stress. A greater number of entanglements inhibited elongation and improved the shear strength. So the increased number of entanglements logically corresponded to the increased shear resistance observed.

Peel and tack tests are better indicators of the stickiness of PSAs but are more complex to analyze than shear resistance tests. They depend significantly on viscous flow during bonding and viscoelastic energy dissipation during debonding. The only differences between loop tack and peel are the contact time and contact force. In peel, 20-min and 24-h dwelling times after an application force of 2 kg are given, whereas in loop tack, separation begins after only 1 s of contact time, and the contact force is given by the bending force of a 50-mm PET film ($\sim$ 10 g).

The results of the tack tests were loop tack force–displacement curves for the three PSA films, as shown in Figure 11. Despite differences in the tack force–displacement curves, the picture patterns were rather similar, which implied a similar micromechanism of adhesive failure. The occurrence of a shoulder after the first initial peak in the curves was characteristic of fibrillation,[24,25] which allowed for significant dissipation of energy.

Dahlquist and Satas[26] correlated tack with the compliance of an adhesive, concluding that good tack was achieved when the compliance was at least 10^{-6} Pa^{-1} after 1 s of compression. This was equivalent to requiring a shear storage modulus of less than 3.3×10^5 Pa at a low frequency because the PSA films had to form bridging fibrils.[27,28] For all PSA films, the modulus values were below that of the Dahlquist criterion, as listed in Table IV, and they all had initial tack forces.

The strength of an adhesive bond is determined by the thermodynamic contributions to the interfacial energy (van der Waals interactions, electrostatic forces, and hydrogen bonding) and the rheological contributions due to the viscoelastic dissipation during deformation of the polymer chains in the adhesive layer itself. The bulk properties dominated the adhesive performance because any difference in the interfacial work of adhesion was small as a result of the overall chemical composition being constant at the growth stage. Although adhesives of low modulus for PSA–BA gave high viscous flow, they did not give high viscoelastic energy dissipation during debonding, as the filament would have fractured rapidly because of a lack of entanglement and a low cohesive strength. Changing the core components from poly(BA) to silica lowered the molecular weight between entanglements and, therefore, created an adhesive with greater cohesive strength. For a PSA with a higher cohesive strength, the resistance to fibril elongation will rise. The tack properties of the PSA–silica film improved, as it was likely to be composed of long and strongly entangled polymer chains. The PSA–MMA film had reasonable tack properties, that is, acceptable wetting of the stainless panel during the contacting step and suitable tack force and tack energy during the debonding process. All of these results were correlated with the structures of the films. Suitable wetting was achieved during the bonding process when dissipation of energy in the bulk of the film was favored during the separation step. As a result, the adhesion and cohesion balance were enough to allow the development of modest tack properties. For PSA–silica, the

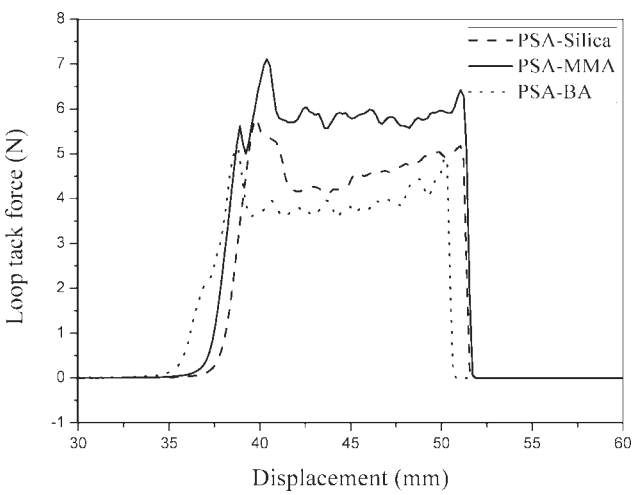

Figure 11 Force–displacement plot for the loop tack measurements.

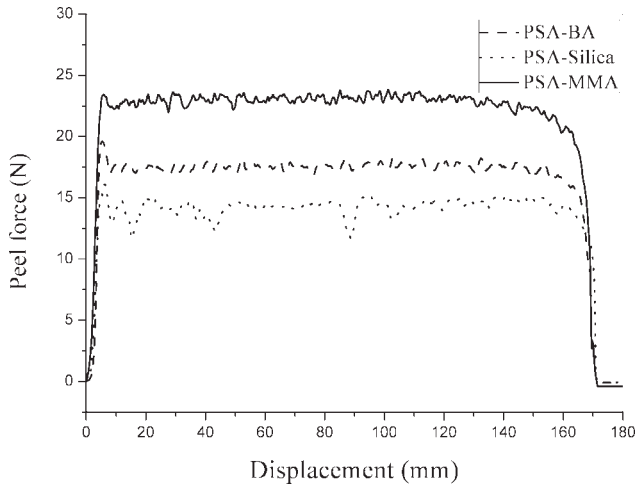

Figure 12 Force–displacement plot for the peel measurements (dwelling time = 24 h).

resistance to fibril elongation rose slightly as it revealed a relatively elastic response. This might have led to a decrease in the intimate contact with the substrate and a medium tack force, although it PSA–silica had the highest cohesive strength. Hence, high viscoelastic energy dissipation was obtained for the PSA–MMA film when there was good anchorage of the adhesive onto the substrate and moderate-modulus/high-elongation fibrils that were deformed during the debonding process, which contributed much to the work of adhesion.

The force measured during peel tests is composed of two components: first, the force that requires the overcoming of the work of adhesion, that is, the breaking of the adhesive/adherent interfacial bond, and second, the force that requires the deformation of the bulk of the adhesive. Figure 12 shows graphically the relationship between the peel force and the adhesives with different core components. As discussed previously, the shell layer polymer, poly(BA-*co*-AA), had sufficient mobility ($T_g = -25°C$) to form a good bond with the substrate at room temperature. Although PSA–BA had a good viscous flow, its cohesive strength was low, which led it to rupture during peeling. For PSA–silica, an increase in the adhesive modulus decreased peel adhesion for two reasons with the increase in modulus of a rubbery polymer due to the incorporation of rigid spheres. First, a decrease in the ability of the adhesive to wet the substrate eventually resulted in a polymer that had no pressure-sensitive properties. Second, as the modulus of the adhesive increased, the amount of adhesive filamentation at the locus decreased, and hence, the volume of adhesive under deformation decreased. This revealed the elastic response because of its highest modulus and did not dissipate high viscoelastic energy during debonding. A high storage modulus, relative to the dissipative character of the adhesive, would induce interfacial crack propagation. The results of the peel tests were the peel force–displacement curves (24 h), shown in Figure 12 (the curves were the same and are not shown for the 20-min dwelling time). Fibrillation, also noticed in peel tests, was observed during the debonding stage, where the initial cavities on the interface grew and were separated by thin fibrils. The failure for the PSA–BA film was the interfacial adhesion type, which corresponded to homogeneous deformation. The failure for PSA–silica and PSA–MMA showed heterogeneous deformation, although adhesion-slip failure sometimes occurred for the PSA–silica film. As deformation continued, air was drawn in from the outside as the outermost fibrils became thinner and broke. The progression led to the formation of separated fibrils and the achievement of a steady-state cross-sectional area. Fibril elongation was facilitated by the decreasing wall thickness and flow from the base of the fibrils during the observed long plateau. The PSA–MMA film had the highest peel force and loop tack. For optimum tack and adhesion, a PSA must not be too stiff and must be able to dissipate energy during deformation.

CONCLUSIONS

The MPS–silica/poly(BA-*co*-AA) composite latex synthesized by semicontinuous emulsion polymerization was used to prepare PSAs. It was easy for the poly(BA-*co*-AA) copolymer to encapsulate on the surface of the seed silica because of the organomodification of the surface on the hydrophilic silica with the MPS silane coupling agent, which resulted in the formation of core–shell structured composite particles. Each MPS–silica particle was enwrapped with polyacrylics during the emulsion polymerization. The narrow-dispersion composite latex of the MPS–silica/poly(BA-*co*-AA) hybrid was obtained after the restricted control of the monomer feed rate and emulsion conditions, and no secondary nucleation occurred. The inclusion of the silicas in the poly(BA-*co*-AA) polymer improved the thermal stability of the resulting PSAs. The time for shear resistance of the MPS–silica/poly(BA-*co*-AA) PSA increased by five times compared with those of poly(MMA-*co*-ALMA)/poly(BA-*co*-AA) and the full poly(BA-*co*-AA) PSAs. This resulted from the increase in cohesive strength within the poly(BA-*co*-AA) PSA with the addition of the modified silica. The reinforcement of the shell-phase polyacrylates by the rigid-core modified silicas yielded an improvement in the viscoelastic properties compared with the others, and the cohesive properties of the adhesive were improved without a decrease in the other adhesive properties. Obviously, such basic studies on acrylic and vinyl modified particles revealed implications to

the optimization of properties of nanofiller-containing adhesives.

The authors thank Peter A. Lovell (University of Manchester, United Kingdom) for many fruitful discussions. The reviewers' comments on this article were very helpful too.

References

1. Benedek, I.; Heymans, L. J. Pressure-Sensitive Adhesives Technology; Marcel Dekker: New York, 1997.
2. Talmage, J. Adhes Technol 2000, 17, 10.
3. Wang, C. L.; Wang, L.; Chen, C.; Chen, T.; Jiang, G. H. J Appl Polym Sci 2006, 101, 1535.
4. Gower, M. D.; Shanks, R. A. J Polym Sci Part B: Polym Phys 2006, 44, 1237.
5. Singa, D. T.; Andew, K. J Appl Polym Sci 2001, 79, 2230.
6. Jovanović, R.; Dubé, M. A. J Macromol Sci Polym Rev 2004, 44, 1.
7. Lovell, P. A.; Shah, T. H. Polym Commun 1991, 32, 98.
8. Chauvet, J.; Asua, J. M.; Leiza, J. R. Polymer 2005, 46, 9555.
9. Howard, J. Adhes Technol 2002, 19, 16.
10. Bourgeat-Lami, E.; Herrera, N. N.; Putaux, J.; Reculusa, S.; Perro, A.; Ravaine, S.; Mingotaud, C.; Duguet, E. Macromol Symp 2005, 229, 32.
11. Liu, W.; Guo, Z.; Yu, J. J Appl Polym Sci 2005, 97, 1538.
12. Wu, T.; Ke, Y. Eur Polym J 2006, 42, 274.
13. Chen, N.; Wan, C.; Zhang, Y. Polym Test 2004, 23, 169.
14. Guo, Y.; Wang, M.; Zhang, H.; Liu, G.; Zhang, L.; Qu, X. J Appl Polym Sci 2008, 107, 2671.
15. Zhang, K.; Chen, H.; Chen, X.; Chen, Z.; Cui, Z.; Yang, B. Macromol Mater Eng 2003, 288, 380.
16. Zhang, K.; Zheng, L.; Zhang, X.; Chen, X.; Yang, B. Colloids Surf A 2006, 277, 145.
17. Mizutani, T.; Arai, K.; Miyamoto, M.; Kimura, Y. Prog Org Coat 2006, 55, 276.
18. Chabert, E.; Bornert, M.; Bourgeat-Lami, E.; Cavaillé, J. Y.; Dendievel, R.; Gauthier, C.; Putaux, J. L.; Zaoui, A. Mater Sci Eng A 2004, 381, 320.
19. Stöber, W.; Fink, A. J Colloid Interface Sci 1968, 26, 62.
20. Shen, H.; Zhang, J.; Liu, S.; Liu, G.; Zhang, L.; Qu, X. J Appl Polym Sci 2008, 107, 1793.
21. Roos, A.; Creton, C. Macromolecules 2005, 38, 7807.
22. Zhao, C. L.; Roser, J.; Heckmann, W.; Zosel, A.; Wistuba, E. Prog Org Coat 1999, 35, 265.
23. Wang, T.; Lei, C. H.; Dalton, A. B.; Creton, C.; Lin, Y.; Fernando, K. A. S.; Sun, Y. P.; Asua, J. M.; Keddie, J. Adv Mater 2006, 18, 2730.
24. Aymonier, A.; Leclercq, D.; Tordjeman, P.; Papon, E.; Villenave, J.-J. J Appl Polym Sci 2003, 89, 2749.
25. Amaral, M.; Roos, A.; Asua, J. M.; Creton, C. J Colloid Interface Sci 2005, 281, 325.
26. Dahlquist, C. A.; Satas, I. Handbook of Adhesives; Van Nostrand Reinhold: New York, 1989.
27. Zosel, A. Colloid Polym Sci 1985, 263, 541.
28. Zosel, A. Int J Adhes Adhes 1998, 18, 265.